PRECIPITATION AND UNDERSTORY VEGETATION DIVERSITY DRIVE VARIATIONS IN SOIL ORGANIC CARBON DENSITY: RESULTS FROM FIELD SURVEYS AND SATELLITE DATA OF TWO DIFFERENT PERIODS IN THE GREATER KHINGAN MOUNTAINS OF NORTHEAST CHINA

LI, F. Z.[1] – LIU, Y.[1,2] – ZHANG, C.[1] – SA, R. L.[1,2] – TIE, N.[1,3*]

[1]Forestry College, Inner Mongolia Agricultural University, Hohhot 010019, Inner Mongolia, China
(e-mail:fengzili@emails.imau.edu.cn, phone:+86-153-2607-5875;ly9810@163.com; zc51study@163.com; sarula213@163.com)

[2]National Field Scientific Observation and Research Station of Forest Ecosystem in Greater Khingan Mountains, Inner Mongolia, Genhe 022350, China

[3]Inner Mongolia Academy of Forestry Sciences, Hohhot 010010, Inner Mongolia, China
(e-mail: wangtieniu@126.com)

[*]Corresponding author
e-mail: wangtieniu@126.com

(Received 2nd Nov 2021; accepted 26th Jan 2022)

Abstract. The forest ecosystem in Greater Khingan Mountains (GKM) is the largest primary forest in northern China. Accurate assessment of the regional carbon (C) pool of soils and analysis of the control factors are essential for setting appropriate forest management policies. Our study was designed to prove the hypothesis that forest soil acts as a C sink owing to continuous C accumulation, which results from constant biomass production within the GKM forests. We investigated topsoil (0-20 cm) C dynamics and diving force in GKM forests (both the Inner Mongolia and Heilongjiang sectors) based on field data from 2000 to 2019. The mean soil organic C density (SOCD) in the topsoil was 10.64 ± 0.83 kg C m^{-2} across the GKM, and the increase rate was 0.15±0.05 kg C m^{-2} y^{-1}. Our results also demonstrated the critical role of precipitation and under vegetation diversity in shaping soil organic C dynamics across the GKM, suggesting that the relationship between the soil C cycle and temperature is unstable in northern ecosystems. Our results provided a new reference range for estimating surface soil C pools in GKM forests ecosystems based on field measurements.
Keywords:*carbon sequestration,spatial variations, carbon–climate feedback,boreal forests, soil inventory*

Abbreviations:GKM: Greater Khingan Mountains; C: Carbon; SOC: Soil organic carbon; SOCD: Soil organic carbon density; SCS: Soil carbon storage; CO_2: Carbon dioxide; N_2O: Nitrous oxide; MAT: Mean annual temperature; MAP: Mean annual precipitation; MGT: Mean growing temperature; MGP: Mean growing precipitation; NDVI: Normalized difference vegetation index; DBF: Deciduous broadleaved forests; DNF: Deciduous needleleaf forests; BNMF: Broadleaved and needleleaf mixed forests; Alt: Altitude; Soil. D: Soil depth; Liiter. D: Litter depth; NH_4^+-N: Ammonium nitrogen concentration; AP: Available phosphorous; AK: Available potassium; Age. Forest: the age of the forests at the individual sampling site

Introduction

Although forests represent just 30% of the land cover, they account for 45% of terrestrial ecosystem C stocks and nearly 50% of terrestrial net primary production (Bonan, 2008). Researchers currently agree that enhancing forest soil C stocks is an effective and environmentally friendly way to absorb carbon dioxide (CO_2) from

http://www.aloki.hu ● ISSN 1589 1623 (Print) ● ISSN 1785 0037 (Online)
DOI: http://dx.doi.org/10.15666/aeer/2003_23032328

anthropogenic emissions (Tharammal et al., 2019; Bossio et al., 2020). Sustainable forest management has been carried out by the Chinese government to protect forest resources, resulting in a significant increase in forest areas from 13.9% (1990s) to 21.0% (2010s) (Tang et al., 2018). Many studies based on field surveys and modeling have assessed the C stocks in forest ecosystems in response to this increase in forest area. The forest topsoil C stock increased significantly from the 1980s to the 2000s, at a rate of increase ranging from 14.1 to 25.5 g C m^{-2} y^{-1} (mean rate of 20.0 g C m^{-2} y^{-1}, 95% confidence) (Yang et al., 2014b). Similar studies found that the forest C stock plays a sink role in China (Yang et al., 2011; Pan et al., 2011; Tharammal et al., 2019). However, soil carbon sink largely depends on the interaction between soil and climate (Crowther et al., 2019). If the soil carbon emission caused by warming exceeds the soil carbon input caused by vegetation growth, the soil ecosystem may become the source of atmospheric carbon dioxide(Schimel et al., 1994; Davidson and Janssens, 2006). It is, therefore, important to obtain an objective understanding of the role played by the forests C balance, to limit global climate warming and to adjust forests management policies (Hopkins et al., 2012).

Environmental factors such as climate and plant diversity, which are directly associated with latitude, limit the distribution power of forest biomass (He, 2012). Interactions and mechanisms among multiple factors (such as climate, site, soil physical and chemical properties, and land use patterns) will affect the distribution of vegetation and soil C storage. The rate of C input and output of the soil is governed by temperature, soil nutrient conditions and atmospheric CO_2 concentrations in the short term (Tian et al., 2011). Decomposition of soil organic matter, the main way in which organic C enters the soil, is frequently affected by ambient temperatures (Davidson and Janssens, 2006). On a national scale, the average annual temperature rise in China was significantly higher thanthe change in global average from 1982 to 2011, exceeding 1°C on average (Fang et al., 2017). These changes will, in turn, feed back into the forest ecosystem in terms of species community (Chen et al., 2018), stoichiometric ratio (Yang et al., 2014a) and ecosystem function in the long term (Crowther et al., 2019). Climate factors are therefore expected to influence the dynamics of soil organic C at large scales.

The area covered by forest in China is vast, at approximately 156 M ha, and it occupies more than one climate zone (Guo et al., 2013). The Greater Khingan Mountains (GKM) forests are mainly distributed in northeastern China and include eastern Inner Mongolia Autonomous Region and northern Heilongjiang Province (Meng et al., 2014; Zhao et al., 2014). These forests are one of the most sensitive ecosystems to global warming (Fu et al., 2018), and forests of the dominant species – *Larixgmelinii* Rupr. (Jiang et al., 2002) - cover more than 57% of the GKM (Bull and Nilsson, 2004; DFPRC, 2014). *Betula platyphylla* Suk. and *Populusdavidiana* are mainly distributed on eastfacing ridges, and *Pinus sylvestris* var. *mongolica* and *Quercus mongolica* form the remaining forest (Bull and Nilsson, 2004; DFPRC, 2014). Like in most high altitude ecosystems, soil stores a huge amount of C due to the long cold season and relatively humid environment in GKM, which provides a better area for analyzing the feedback between soil C and climate change. Two studies of forest C storage in GKM (including both Inner Mongolia and Heilongjiang Province in northeastern China) have suggested that the forest C stock acts as a C sink (Meng et al., 2014; Zhao et al., 2014). In contrast, a recent study based on the InVEST model showed that the soil stock is stable while ecosystem C stock has experienced a slight decrease in northeastern China (Mao et al., 2019). However, due to the limited data and difficult large-scale field survey in GKM area, there is little research

http://www.aloki.hu ● ISSN 1589 1623 (Print) ● ISSN 1785 0037 (Online)
DOI: http://dx.doi.org/10.15666/aeer/2003_23032328

on the historical dynamics of SOC in GKM. How the soil C pool of the GKM responds to increased climate change remains uncertain.

In order to detect the change of soil carbon storage in GKM, 204 soil profiles were obtained from 68 sites of GKM. We compared our 68 field surveys obtained in 2017 (representing data from the 2010s) with 107 field surveys published in 2000-2010 (representing data from the 2000s) (Xu et al., 2018a). Since plant production is the main C input of soil in terrestrial ecosystems, satellite data sets which can reflect vegetation growth have been general used to evaluate aboveground biomass(Shen et al., 2015; Zhang et al., 2016). And many studies have shown that the satellite data set can be combined with ground observation data to estimate regional SOC reserves (Yang et al., 2008, 2009; Ding et al., 2016). Therefore, based on the satellite-based SOC estimation method, we analyzed the historical changes of SOC in GKM forests by comparing the data of current measurements (2010s) and historical literature published (2000s). The specific objectives of this research were as follows: (1) based on field survey and satellite data set, to verify the hypothesis that soils of GKM forests can function as C sinks in the regional C cycle because of the underlying C accumulation in vegetation biomass in the 2000s and 2010s (Pan et al., 2011; Fang et al., 2012; Yang et al., 2014b); and (2) analyze the factors influencing SOCD both in spatial distribution and long term scale. Application of our results is expected to improve C sequestration budgets, and thus contribute to sustainable forest management.

Materials and Methods

Data sources

The 2010s soil sampling was conducted between June and August 2017 in GKM, China (geographical range is 119°36′-125°19′E, and 47°3′-53°20′N) (Liu et al., 2020). We defined "forests" as an area of land > 0.067 ha that is dominated by trees and with a canopy density of > 0.2 (Tang et al., 2018). According to the system sampling method, 56 sampling points were set in a 0.5° × 0.5° (~60×60 km) grid. Temporary standard plots were visually uniform, well populated stands of > 1 ha; at least 100 m from any openings to minimize the impact of edge effects; and round, with a radius of 17.5 m (or 500.34 m^2). To allow analysis of the soil properties, five pits were dug along an "s" route in each temporary standard plot to collect topsoil (0-20 cm) samples, so that sampling points were more representative (Zhu et al., 2020). The soil samples were manually selected to remove fine roots of plants for properties analysis, passed through a 2 mm sieve, and then divided into three parts. One sample was dried at a constant temperature of 105°C for measuring bulk density. The other sample stored at 4°C was extracted with 1 M KCl solution, and then analyzed using a flow injection analyzer (Autoanalyzer 3 SEAL, Bran and Luebbe) for NH_4^+-N concentrations. The third sample Air-dried were extracted with 0.03 M NH_4F and 0.025 M HCl, and analyzed colorimetrically to determine available P concentrations using vanado-molybdate method (Bray and Kurtz, 1945).Soil pH was determined in a 1:5 soil to deionized water suspension using a pH probe (PB-10, Sartorius).Additionally, the average rock content (> 2 mm) of each soil type was replaced by the same soil type (Zhu, 1996). In 2019 we supplemented our 2017 work with samples taken from 12 points in the central GKM, using the same plot setting and soil survey methods. This gave us a total of 68 soil samples were used as soil data for 2010s (*Fig. 1*, *Table A1*). The age of the forest at the individual sampling site was obtained from the satellite images that developed a top-down method to downscale the provincial statistics

http://www.aloki.hu ● ISSN 1589 1623 (Print) ● ISSN 1785 0037 (Online)
DOI: http://dx.doi.org/10.15666/aeer/2003_23032328

of national forest inventory data into 1km stand age map using climate data and Light Detection And Ranging (LiDAR) derived forest height (Zhang et al., 2017).

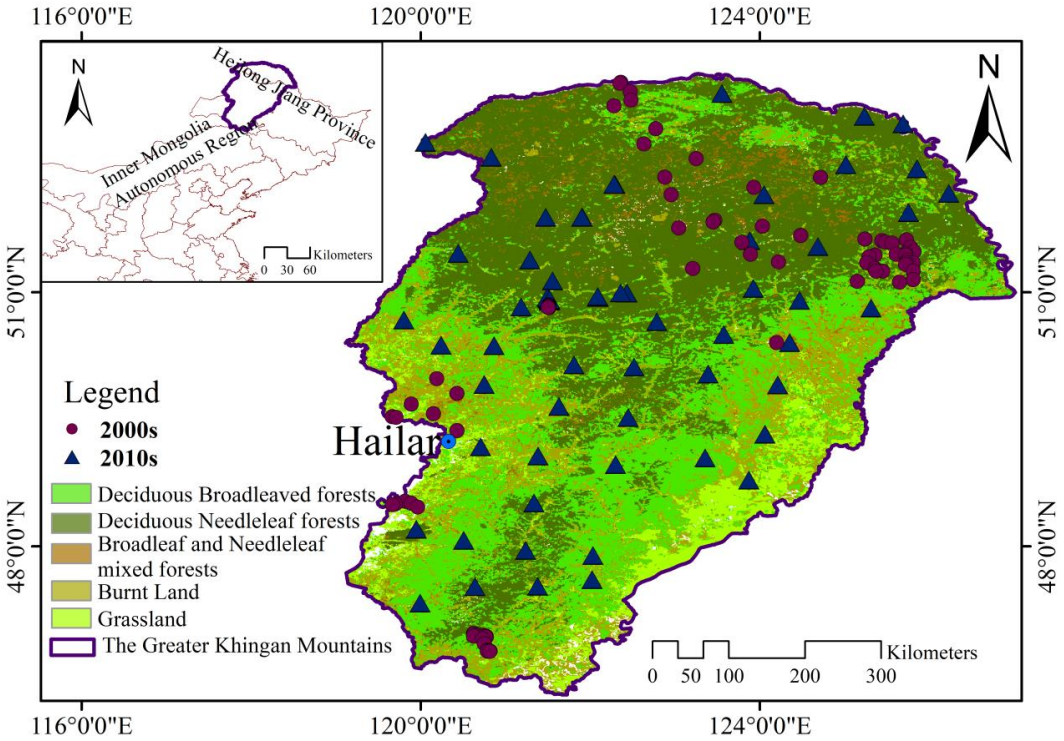

Figure 1. *Locations of the sampling sites of the two periods (2000s and 2010s) in the Greater Khingan Mountains, northeastern China. Solid purple dot, 2000s; solid blue triangle, 2010s*

The SOCD of 2000s soil was selected from the "2010s China Land Ecosystem Carbon Density Dataset" (Xu et al., 2018a), which lists SOCD from field surveys in 2004-2012. Selection of the soil data was based on (1) experiments conducted in 2000-2009 with no restriction on publication year; and (2) experimental sites in the forest ecosystem of the GKM (according to latitude and longitude coordinates) and soil depths of 0-20 cm. We used a total of 107 observations of soil samples to represent the 2000s.

Environmental factors have traditionally been used to represent the changes in the soil C cycle across landscapes (Crowther et al., 2019). We used the annual variations in temperature and precipitation to analysis the climate change trend at regional level in the GKM during 1981 to 2019. Mean annual temperature (MAT, °C), mean annual precipitation (MAP, mm), mean growing temperature (MGT, °C) and mean growing precipitation (MGP, mm) for each sites were calculated using CRU_ts4_pre and CRU_ts4_tmp datasets, CRU TS provides 0.5° resolution monthly data covering the global land surface from 1901 to 2020, provided by the National Centre for Atmospheric Science (NCAS) in the United Kingdom (https://crudata.uea.ac.uk/cru/data/hrg/).

Annual variation in the remotely sensed normalized difference vegetation index (NDVI) was used to explore the vegetation growth trend at regional level in the GKM. The NDVI data set was obtained from the GIMMS NDVI3g dataset with the spatial resolution of 8 km from 1982 to 2015 (https://ecocast.arc.nasa.gov/data/pub/gimms/), and Moderate Resolution Imaging Spectroradiometer (MODIS) through the United States Geological Survey (USGS; http://modis.gsfc.nasa.gov), with a spatial resolution of 250 m

http://www.aloki.hu ● ISSN 1589 1623 (Print) ● ISSN 1785 0037 (Online)
DOI: http://dx.doi.org/10.15666/aeer/2003_23032328

for every 16 day interval over the 2000-2019 (MOD13Q1) (Tucker et al., 2004, 2005). Monthly composites were obtained by application of the maximum value composition (MVC) method (Holben, 1986). The NDVI data were selected from GIMMS NDVI3g dataset from 1982 to 1999 and MOD13Q1 from 2000 to 2019.

Data processing

Soil C is mainly distributed at depths of 0-100 cm; is concentrated at depths of 0-20 cm; and decreases as soil depth increases (Crowther et al., 2019). The soil organic C density (SOCD) and soil C storage (SCS) in the top 20 cm were calculated by *Eq.1*and *Eq.2*:

$$SOCD = \sum_{i=1}^{n} SOCi \times BDi \times Ti \times (1 - Ci)/100 \quad \text{(Eq.1)}$$

where *SOCD*, *SOCi*, *BDi*, *Ti* and *Ci* represent soil organic C density (kg C cm^{-2}), soil organic C (g kg^{-1}), bulk density (g cm^{-3}), layer thickness (cm) and percentage of the fraction > 2 mm, respectively; and:

$$SCS = SOCDi \times Ai \quad \text{(Eq.2)}$$

where *SCS*, *SOCDi* and *Ai* represent soil C storage (Pg C), soil organic C density (kg C cm^{-2}) and area (m^2), respectively.

Forest types in 2010s field survey were distinguish according to the principles and bases of Chinese vegetation regionalization, which defined the: deciduous broadleaved forests (DBF, deciduous broadleaved species stock accounts for more than 80% of stand stock), deciduous needleleaf forests (DNF, deciduous needleleaf species stock accounts for more than 80% of stand stock) and broadleaf and needleleaf mixed forests (BNMF, Coniferous or broad-leaved trees account for 20% to 80% of stand stock)(Chinese Academy of Sciences, 2001; Ministry of ecology and environment of the people' s Republic of China, 2021).Forest types in 2000s dataset were distinguish according the global land cover data (GlobalLandCover30, second-class product data, with a spatial resolution of 1 km) (http://www.globallandcover.com).Different forest types area using the raster statistical function of ArcGis (ArcGis 10.2.2, ESRI).

To examine understory vegetation diversity, we selected four indices of *αlpha* diversity. These focus on measuring the number of biological species in the community and reflect the coexistence results of species through competition for resources in the community (Wu, 2015). The calculation formulae(Chen and Zhang, 1999) are*Eq.3-Eq.6*:

$$\text{Shannon–Wiener indices: } H = -\sum_{i=1}^{S} P_i ln\, P_i \quad \text{(Eq.3)}$$

$$\text{Simpson diversity indices: } P = 1 - \sum_{i=1}^{S} P_i^2 \quad \text{(Eq.4)}$$

$$\text{Pielou evenness indices: } E = H' / ln\, S \quad \text{(Eq.5)}$$

$$\text{Margalef indices: } D = \frac{S-1}{ln\, N} \quad \text{(Eq.6)}$$

http://www.aloki.hu ● ISSN 1589 1623 (Print) ● ISSN 1785 0037 (Online)
DOI: http://dx.doi.org/10.15666/aeer/2003_23032328

where S is the total number of species for each sample, N is the sum of all important values for S species; and P_i is the important value of the first species. Creation of an understory vegetation diversity indices was performed in R (4.0.3) using the "vegan" package.

Statistical analyses

Sen + Mann-Kendall trend analyses were used to analyze changes in NDVI over the past 20 years (2000-2019)(Liu, 2017). A method for longtime series trend analysis can be created by combining the trend degree in the Sen slope estimator method with the trend degree test in the Mann-Kendal method, and the latter has become an important method to judge the trend of longtime series data(Gocic and Trajkovic, 2013).

The time series length of this study was 10 year (2000-2009, 2010-2019), so the Mann-Kendall Z trend test (Z_{MK} test) was used to test statistics. The Z_{MK} test trend criterion was based on *Table 1*(Seenu and Jayakumar, 2021). We performed the Sen + Mann-Kendall trend analyses using MATLAB (2016).Take into account the influence of grassland and farmland distribution, We extracted forest areas from Sen+Man-Kendall results of NDVI according to the satellite images on a 1:1 million vegetation map of China (Hou, 2019)(http://data.tpdc.ac.cn). Then recalculated the area and proportion of different types.

Table 1. *Normalized difference vegetation index (NDVI) trend analysis results of the Sen + Mann-Kendall method with a confidence interval of 95%*

NDVI Trend	Rating	2000s		2010s		Change in NDVI	
		Area (10^4 m^2)	Percent %	Area (10^4 m^2)	Percent %	Area (10^4 m^2)	Percent %
$\beta < 0$, $\|Z\| > 1.96$	Decreased obviously	0.03	0.14	0.01	0.05	-0.02	-0.09
$\beta < 0$, $\|Z\| \leq 1.96$	Decreased slightly	4.78	25.34	0.40	2.12	-4.38	-23.21
$\beta > 0$, $\|Z\| \leq 1.96$	Increased slightly	12.61	66.80	6.35	33.66	-6.25	-33.14
$\beta > 0$, $\|Z\| > 1.96$	Increased obviously	1.45	7.71	12.10	64.16	10.65	56.45

In order to analyze the SOCD dynamics, we compared the SOCD changes in the two periods both in field survey and satellite estimation. SOCD based on field survey is calculated by *Eq. 1* and *Eq. 2*. Single factor analysis of Variance (ANOVA) was conducted to determine whether SOCD derived from field survey differed significantly during the 2000s and 2010s in different forest types. The effect of two periods (2000s and 2010s) was considered significant if $P < 0.05$. ANOVA was carried out using the "vegan" package in R version 4.0.3.

SOCD based on satellite estimation is estimated by obtaining the polynomial regression relationship between NDVI and SOCD. Polynomial regression model is a kind of linear regression model, in which the regression function is linear about the regression coefficient(Schmidt et al., 2013; Zhang et al., 2014).Vegetation indices commonly used in terrestrial ecosystem research include normalized difference, enhancement, soil adjustment and modified soil adjustment vegetation indices(Zhang et al., 2016). NDVI has been widely used in inversion of terrestrial vegetation and terrestrial ecosystem carbon dynamics(Yang et al., 2008, 2009; Ding et al., 2016).We use the polynomial regression relationship between SOCD and the corresponding NDVI data to obtain the SOCD spatial distribution maps of the two periods (2000s and 2010s). Then the paired t-test was used to compare the changes of SOCD in the two periods from the grid level. Finally, the SOCD difference of each grid in the two periods is calculated, and the

http://www.aloki.hu ● ISSN 1589 1623 (Print) ● ISSN 1785 0037 (Online)
DOI: http://dx.doi.org/10.15666/aeer/2003_23032328

distribution map of SOCD changes from 2000s to 2010s is obtained. The NDVI data details of this part could be found in the "data source" above in this paper. In addition, reduce the influence of bare soil, water and construction land grid on the simulation results, the grid units with annual NDVI < 0.1 in 20 years were removed for analysis(Piao et al., 2006). In order to verify the reliability of SOCD based on NDVI estimation, we randomly selected 75 % of the soil samples to establish the relationship between SOCD density and NDVI, and then the remaining 25 % were verified. Polynomial regression and the paired t-test were performed in ~~in~~ R version 4.0.3, paired t-test was carried out using the "dplyr" package.

We used redundancy analysis (RDA) to decompose the spatial variation in SOCD into variation related to environmental variables (Alt (m); MAP (mm); MAT (°C); Soil depth (cm); Litter depth (cm); Age. Forest (year); $NH4^+$-N (mg g^{-1}); AP (mg g^{-1}); AK (mg g^{-1}); under vegetation diversity: Margalef, Shannon-Wiener, Simpson diversity and Pielou indices). Further the multiple regression was performed to assess the relative importance of each environmental variable in different forests types based on standardized regression coefficients. Multiple linear regression analysis was used to simulate the relationship between SOCD and climate (MAP (mm); MAT (°C)) at grid level during the 2000s and 2010s. The SOCD map based on NDVI estimation was resample so that the same resolution as climate data. RDA was carried out using the "vegan" package in R version 4.0.3. Multiple linear regression analysis was performed in R version 4.0.3.

Results

Climate change and NDVI trend analysis from 1981to 2019

Climate change in 1981 to 2019

From 1982 to 2019, the annual average NDVI showed a significant increase trend with fluctuated between 0.33 and 0.40 (P <0.05). From 1981 to 2019, MAT has a significant increase overall, with an annual average temperature of -3.67 °C to -1.31 °C (P < 0.05). MAP showed a slight downward trend with an annual average precipitation of 330.12 mm to 571.85 mm, but did not reach a significant level (P > 0.05) (*Fig. 2*).

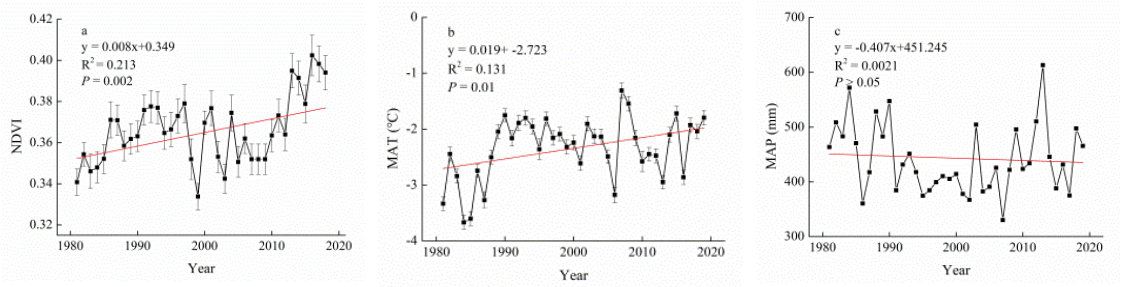

Figure 2. *Annual trends of NDVI, precipitation and temperature in 1981-2019*

From 1982 to 2019, the NDVI in growing season showed a significant increase trend with fluctuated between 0.42 and 0.53 (P < 0.05). From 1981 to 2019, MGT increased significantly, with an average temperature of 9.67 °C to 11.98 °C (P < 0.05). MGP showed a slight downward trend with an average precipitation of 285.68 mm to 558.62 mm, but did not reach a significant level (P > 0.05) (*Fig.3*).

http://www.aloki.hu ● ISSN 1589 1623 (Print) ● ISSN 1785 0037 (Online)
DOI: http://dx.doi.org/10.15666/aeer/2003_23032328

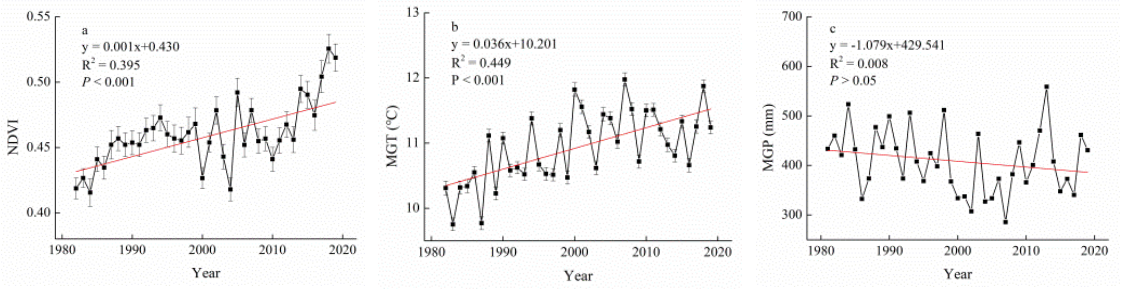

Figure 3. *Trends of NDVI, precipitation (mm) and temperature (°C) in growing season in 1981-2019*

NDVI trend analysis

The spatial distribution characteristics of forest vegetation change trend in the GKM, based on the Sen + Mann-Kendall tests (implemented as shown in *Table 1*), were obtained for the 2000s (2000-2009) and 2010s (2010-2019) (*Fig.4*). From 2000 to 2009 the vegetation change trend in the GKM increased overall, and the area of vegetation change with an upward trend reached 74.51%. The NDVI increased in the north, east and south of the GKM, and decreased in the west and southeast (*Fig. 4*). From 2010 to 2019, the trend in vegetation change of GKM increased overall, and the area showing a rising trend reached 97.82%. There was a large increase in the central and western parts of the GKM, and a downward trend in the eastern part (*Fig.4*).

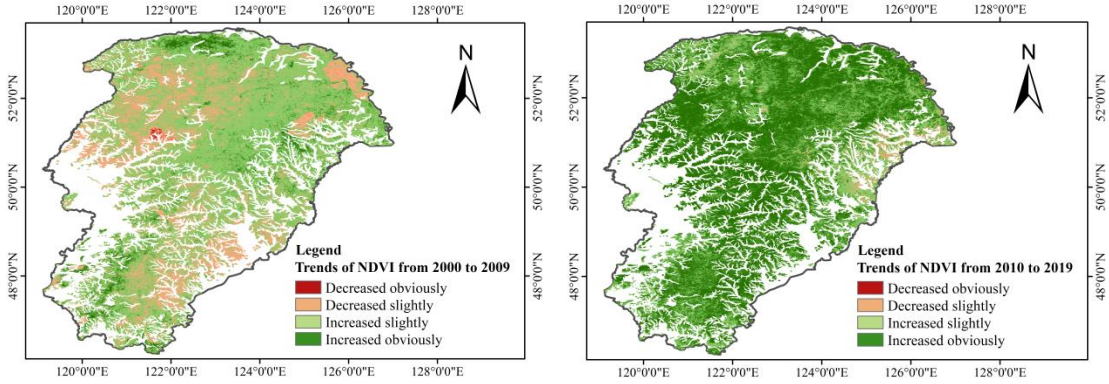

Figure 4. *Trends of inter-annual normalized difference vegetation index (NDVI) from 2000 to 2009 and 2010 to 2019*

Table 1 shows the Z value level based on the Sen + Mann-Kendall test, and the NDVI change trend and area of the two periods (2000s: 2000-2009; 2010s: 2010-2019). From 2000 to 2009, 7.71% of the vegetation of the area significantly improved, 66.80% of the area slightly improved, 25.34% of the area degraded slightly and 0.14% of the area was clearly degraded, indicating that the vegetation trend increased during 2000-2009. From 2010 to 2019, 64.16% had a significant improvement in vegetation, 33.66% had a slight improvement, 2.12% had a slight degradation and 0.05% of the GKM showed significant degradation, indicating that the vegetation trend increased during 2010-2019. Overall, the NDVI increased significantly by 56.45% between the 2000s and 2010s (*Table 1*).

http://www.aloki.hu ● ISSN 1589 1623 (Print) ● ISSN 1785 0037 (Online)
DOI: http://dx.doi.org/10.15666/aeer/2003_23032328

Dynamics of SOCD across the GKM in the 2000s and 2010s

Dynamics of SOCD based on field survey

Based on the dataset of 2000s (Xu et al., 2018a)and 2010s (this study), the average SOCD at 0-20 cm depth in the 2000s and 2010s was 9.15 ± 0.36 kg C m^{-2}(Xu et al., 2018a)and 10.64 ± 0.83 kg C m^{-2}(this study), respectively. The SCS (soil C storage) in the surface layer (0-20 cm) of GKM in the 2000s and 2010s was 2.91±1.14 Pg C (Xu et al., 2018a)(Pg = 10^{15}g) and 3.38 ± 2.63 Pg C (this study), respectively (*Table A2*). The surface SOCD in GKM increased significantly from the 2000s to the 2010s, and the mean increase rate was 0.15 ± 0.05 kg C m^{-2} y^{-1} ($P < 0.05$). In DBF the average increase was 0.34 ± 0.12 kg C m^{-2} y^{-1} ($P < 0.05$). The increase in BNMF and DNF did not reach a significant level, and the increase rates were 0.26 ± 0.15 kg C m^{-2} y^{-1} ($P > 0.05$) and 0.03 ± 0.009 kg C m^{-2} y^{-1} ($P > 0.05$), respectively (*Fig. 5*).

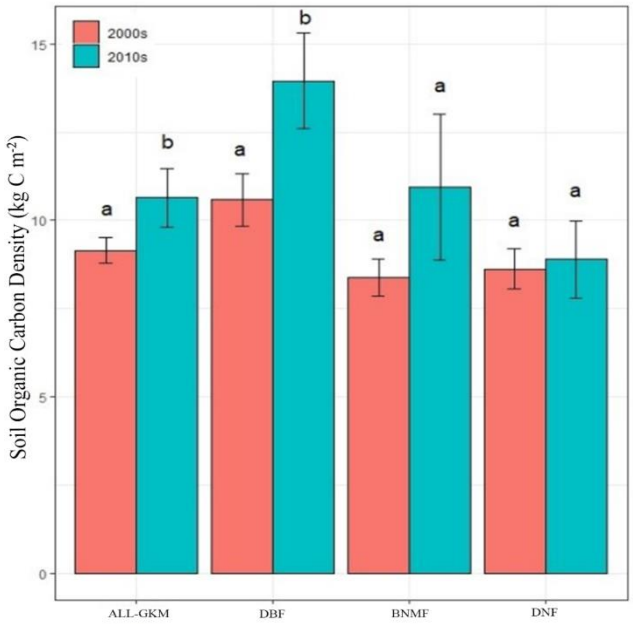

Figure 5. *Soil organic carbon density (kg C m^{-2}) of different periods and forests types at a confidence interval of 95%. The same letter indicates that the statistical test is not significant (P > 0.05). Vertical bars represent the standard error of the mean*

Dynamics of SOCD based on NDVI estimation

*Table 2*shows the parameters of SOCD estimated by polynomial regression based on NDVI, where Adj.R> 0.5 and P < 0.001, indicating that the polynomial regression relationship based on NDVI can better invert SOCD (*Fig. A1*).

Table 2. *Polynomial regression results of soil organic carbon density (SOCD, kg C m^{-2}) and normalized difference vegetation index (NDVI)*

	Summary					ANOVA		
	Intercept/SE	**B1/SE**	**B2/SE**	**Adj.R^2**	**RMSE**	**n**	**F**	**P**
2000s	-10.20/3.32	73.06/18.36	-48.74/24.48	0.68	2.13	107	115.19	***
2010s	-13.90/6.33	96.65/37.30	-66.15/52.46	0.53	4.70	50	27.55	***

***: P<0.001, at a 95% confidence interval

http://www.aloki.hu ● ISSN 1589 1623 (Print) ● ISSN 1785 0037 (Online)
DOI: http://dx.doi.org/10.15666/aeer/2003_23032328

The results showed that there was a significant correlation between the simulated SOCD and the measured SOCD (Adj.R^2 = 0.81, Adj.R^2 = 0.71, P < 0.001, *Fig. 6*). Therefore, based on NDVI, we choose polynomial regression method to develop SOCD of GKM.

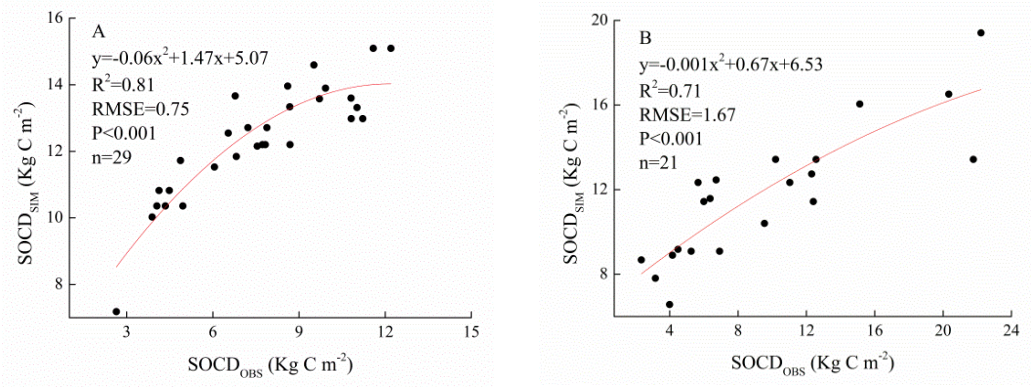

Figure 6. *Correlation between simulated and measured soil organic carbon density ($SOCD_{SIM}$; $SOCD_{OBS}$; kg C m^{-2}) in the Greater Khingan Mountains for the period of 2000s (A) and 2010s (B), derived from polynomial regression*

Based on NDVI estimation, the spatial distribution of SOCD varies greatly in two periods, and the SOCD change shows large spatial heterogeneity (*Fig. A2*). According to the paired t-test results (*Table 3*), SOCD increased by 0.32± 0.001 g C m^{-2} yr^{-1} on average from 2000s to 2010s (P < 0.001).

Table 3. *The paired t-test results of Soil organic carbon density (SOCD, kg C m^{-2}) difference comparison between 2000s and 2010s*

	Summary				
	change in SOCD	**Conf. int**	**t**	**df**	**P**
2000s-2010s	-3.21	-3.21, -3.20	-993.74	991437	***

Conf. int: at a 95% confidence interval; ***: P<0.001

Due to the limitation of data resolution and the large range of study area, SOCD changes are not analyzed at different forests types. According to different forests regions of GKM, SOCD change was compared. It can be seen that from 2000s to 2010s, the increase of SOCD was mainly concentrated in the northeastern and northern forest regions, while the eastern and southern forest regions showed a flat state of increase and decrease (*Fig. 7*). The above results show that the SOCD storage increase in the south of GKM is lower than that in the north of GKM from 2000s to 2010s.

Impact factors of SOCD

The SOCD of the in the GKM forests showed a great change in spatial distribution, ranging from 1.22 to 28.22 kg C m^{-2} (*Fig. A3*). The average SOCD was 10.64 ± 0.83 kg C m^{-2}. Among the three forests types (*Fig. 8A*), DBF (13.95 ± 1.35 kg C m^{-2}) had the highest SOCD, followed by BNMF (10.94 ± 2.05 kg C m^{-2}), DNF (8.89 ± 1.10 kg C m^{-2}) had the lowest SOCD. Across the GKM forests area (*Fig. 8B*), the SOCD

http://www.aloki.hu ● ISSN 1589 1623 (Print) ● ISSN 1785 0037 (Online)
DOI: http://dx.doi.org/10.15666/aeer/2003_23032328

of southern (13.83 ± 1.96 kg C m^{-2}) and eastern (13.11 ± 1.55 kg C m^{-2}) areas were the highest, and the central forest area (3.80 ± 0.69 kg C m^{-2}) was the lowest.

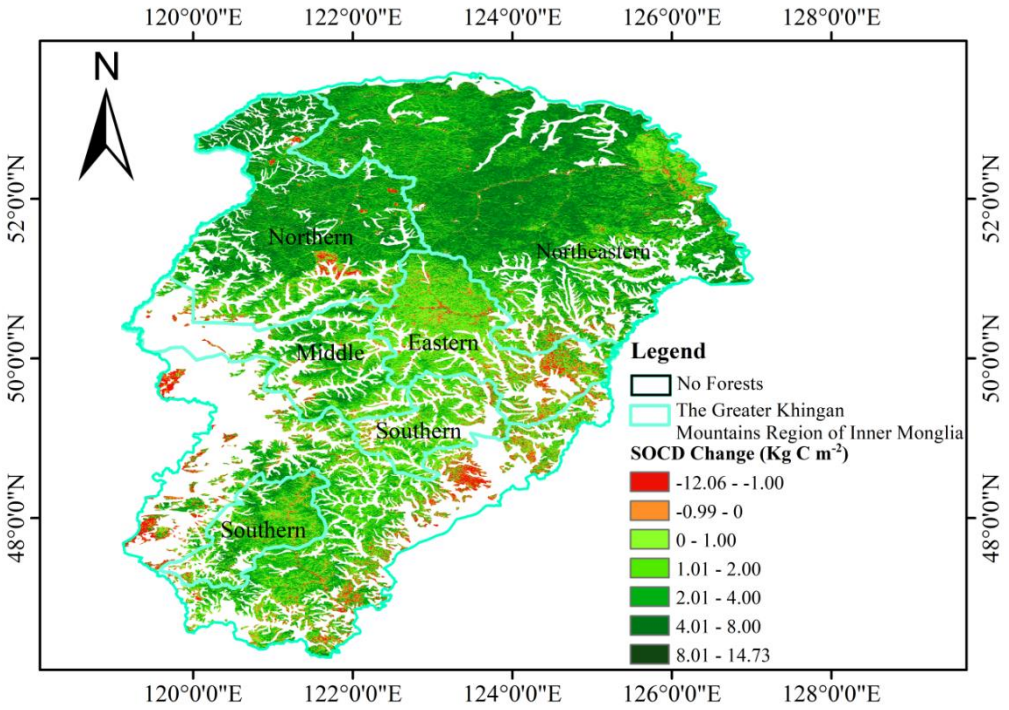

Figure 7. *Soil organic carbon density (kg C m^{-2}) changes in the Greater Khingan Mountains between 2000s and 2010s*

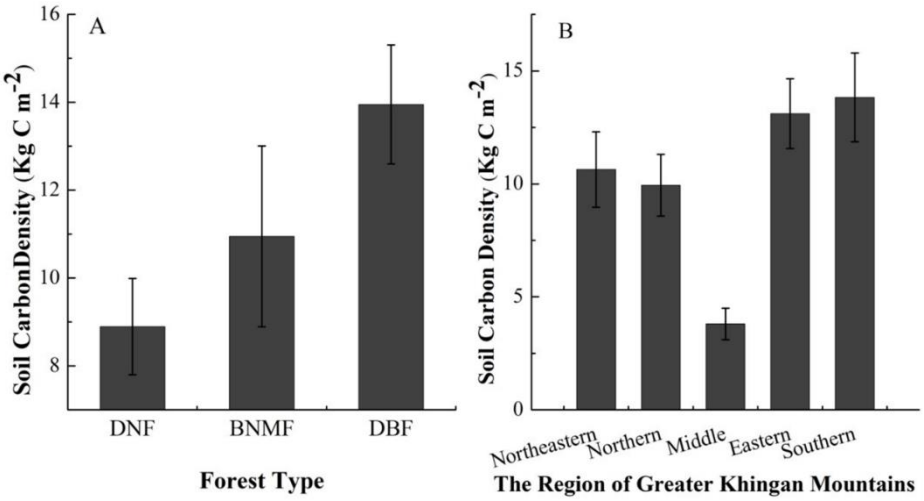

Figure 8. *Soil organic carbon density (kg C m^{-2}) of different forests types and regions*

We used RDA to investigate the relationship between topsoil SOCD and environmental and under vegetation diversity (*Fig. 9*). RDA1 and RDA2 explained 15.82% and 4.91% of the total variation, respectively. The length of arrows indicated that soil depth, Shannon-Wiener indices, Simpson indices, MAT and MGT were the most

http://www.aloki.hu ● ISSN 1589 1623 (Print) ● ISSN 1785 0037 (Online)
DOI: http://dx.doi.org/10.15666/aeer/2003_23032328

important environmental factors affecting SOCD. In contrast, the slope and Soil depth had no significant effect on SOCD. Altitude and slope were nearly vertical in orientation, indicating that they affected SOCD independently, and the influence of these two factors was more reflected in DNF. The angle between SOCD and pH or MAP was acute, indicating that the SOCD was closely positively correlated with these two factors.

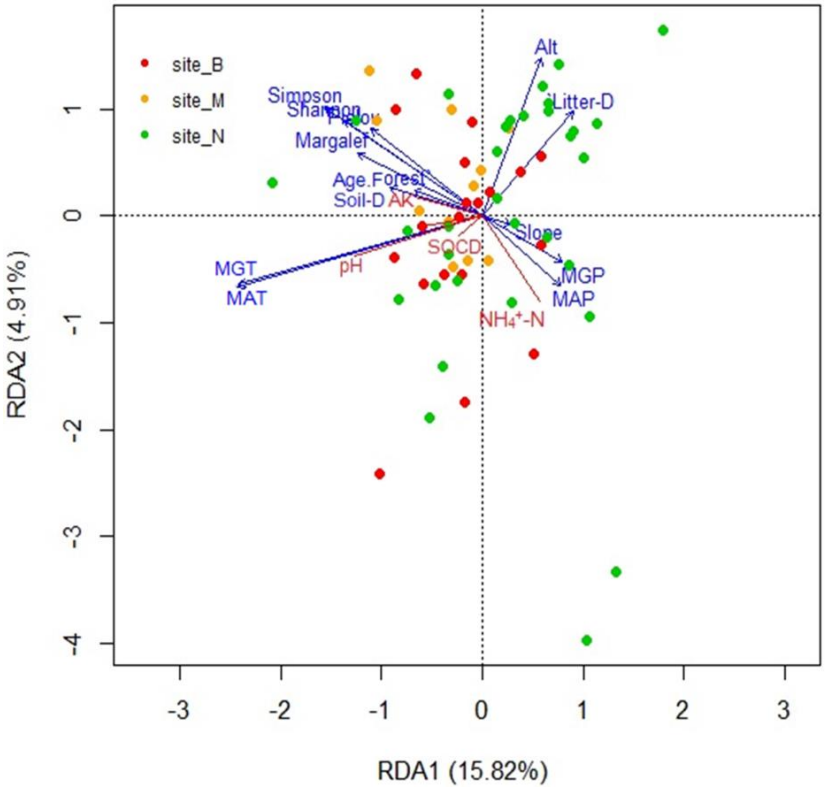

Figure 9. *Redundancy analysis (RDA) of soil organic carbon density (SOCD, kg C m^{-2}) indicators and environmental factors. site_B, deciduousbroadleavedforest; site_M, broadleaf and needleleaf mixed forest; site_N, deciduousneedleleafforest*

Multiple regression was used to quantitatively analyze the relative importance of site, soil nutrients, climate and under vegetation diversity on SOCD in different forests types. The results showed that the SOCD of DNF and DBF was affected by both biotic and abiotic factors, but that the SOCD of BNMF was mainly affected by abiotic factors (*Fig. 10*). Multiple regression models explained 31.8%, 98.8% and 52.5% of SOCD variation in DNF, DBF and BNMF, respectively. We found, using the standardized regression coefficient and its P value, that the slope and Pielou indices had a considerable negative effect on SOCD in DNF ($P < 0.05$). Other variables with large (but not significant) effects included the Simpson indices (positive effect), Shannon indices (negative effect), MAP (positive effect) and MGP (negative effect) ($P > 0.05$). The pielou indices, Shannon indices and MGP significantly promoted changes in SOCD in DBF ($P < 0.05$); while the Simpson indices, Margalef indices, and MAP, had significant negative effects ($P < 0.05$). Abiotic factors had a great influence on soil nutrients in BNMF. Of these, litter depth had a considerable negative effect on SOCD ($P < 0.05$), while NH_4^+-N and AP had relatively small but significant effects ($P < 0.05$).

http://www.aloki.hu ● ISSN 1589 1623 (Print) ● ISSN 1785 0037 (Online)
DOI: http://dx.doi.org/10.15666/aeer/2003_23032328

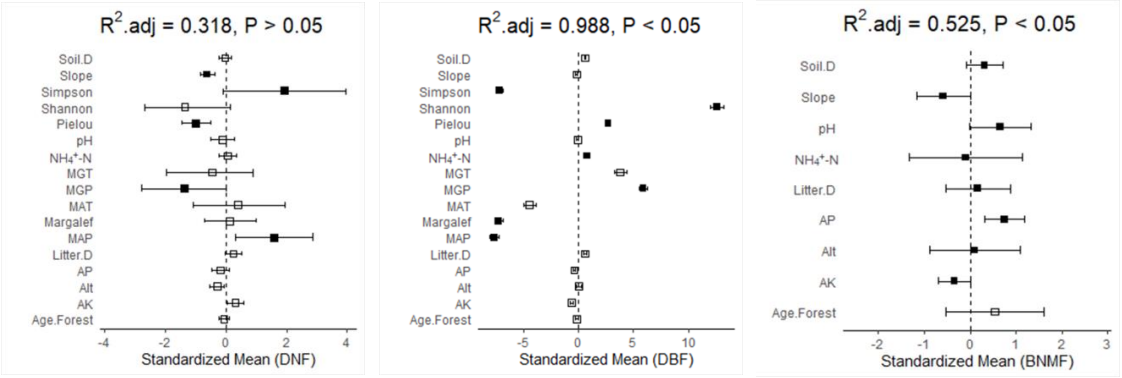

Figure 10. *Multiple regression of abiotic and biotic factors affecting soil organic carbon density (SOCD, kg C m^{-2}) in three different forests types. The points in the figure represent the mean of the standardized regression coefficient, the error bars represent the standard error and the solid points indicate variables that have significant effects on soil organic carbon density (P < 0.05)*

Correlation analysis between SOCD and MAP and MAT in two periods based on NDVI estimation. Multiple linear regression shows, the SOCD dynamics showed a positive correlation with MAP both in 2000s and 2010s, but a negative relationship in 2000s and weak relationship in 2010s with MAT (*Fig. 11*). The results showed that due to the increase of temperature in recent years, the limiting effect of precipitation on SOCD was enhanced(*Table A3.* $Estimate_{MAP2000S}$=0.29, P<0.01; $Estimate_{MAP2010S}$=0.56, P < 0.001), and the effect of MAT was weakened(*Table A3.* $Estimate_{MAT2000S}$=-0.24, P <0.01; $Estimate_{MAT2010S}$=-0.001, P>0.05).

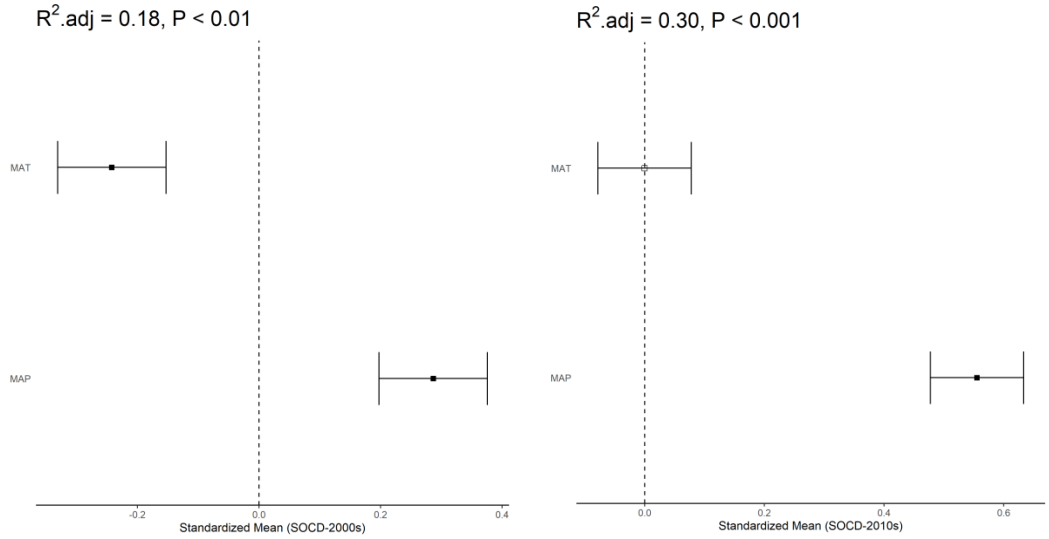

Figure 11. *Correlation analysis between SOCD and MAP and MAT in two periods based on normalized difference vegetation indexestimation, derived from multiple linear regression. The points in the figure represent the mean of the standardized regression coefficient, the error bars represent the standard error and the solid points indicate variables that have significant effects on soil organic carbon density (P < 0.05)*

http://www.aloki.hu ● ISSN 1589 1623 (Print) ● ISSN 1785 0037 (Online)
DOI: http://dx.doi.org/10.15666/aeer/2003_23032328

Discussion

Dynamics of SOCD

Accurate estimation of the soil C pool size is crucial for assessing the function of soil in the global C cycle, particularly in cold temperate forest where approximately 48% of C is stored in the top 30 cm of soil(Yang et al., 2007). The average SOCD in the surface soil (0-20 cm) in the GKM was 10.64 ± 0.83 kg C m^{-2} (*Table A2*), which was close to the whole China forests mean SOCD (11.53 ± 2.24 kg C m^{-2}) reported by Xu et al.(2018b). Our result was lower than the whole China forests mean SOCD (16.38 ± 8.4 kg C m^{-2}) reported by Tang et al.(2018), and this may have been because of the extensive area of young forests and frequent disturbance activities leading to a lower biomass in GKM (Fang et al., 2007). The mean SOCD in different forests types changed from 9.15 ± 0.36 to 10.64 ± 0.83 kg C m^{-2} over the 2000s to the 2010s, and the mean rate of increase was 0.15 ± 0.05 kg C m^{-2} y^{-1} ($P < 0.05$, *Table A2*). This trend of increase was also observed in DBF ($P < 0.05$), but not obvious in BNMF ($P > 0.05$) and DNF ($P > 0.05$, *Table A2*).

The results based on field survey showed that, in GKM, SOCD increased significantly in the period 2000s-2010s (*Fig. 5*, $P < 0.001$). Our results showed that the gross regional scale change in topsoil SOCD ranged from 0.03 ± 0.009 to 0.34 ± 0.12 kg C m^{-2} y^{-1}. Furthermore, the change in rate of SCS in the topsoil ranged from 0.04 to 0.48 Tg C y^{-1} (Tg = 10^{12} g) from the 2000s to the 2010s. The paired t - test results showed that, SOCD based on NDVI estimation increased significantly in the period 2000s-2010s in GKM (*Table 3*; $P < 0.001$), with a mean increased rate of 0.32±0.0001 kg C m^{-2} y^{-1} (mean SOCD of 11.60±0.0001 kg C m^{-2} in 2000s and 14.17±0.0001 kg C m^{-2} in 2010s, *Table A4.*). And the SOCD change difference results show that (*Fig. 7*), SOCD mainly increases in the north of GKM more than in the south, which may be due to the wide distribution of the old forests in the north of GKM, less human disturbance, which is conducive to the accumulation of SOCD(Mao et al., 2019).In the south of GKM, human activities are frequent, especially a large number of plantation activities. The establishment and management of plantations often involve serious human disturbances, such as deforestation and intense land preparation, which may lead to rapid and substantial soil organic carbon losses and affect longterm soil organic carbon recovery(Yang et al., 2019).

The C store in GKM forests topsoil may be ascribed to its natural accumulation in mineral soil during forest development. The increased NDVI we observed in this study could be interpreted as demonstrating this hypothesis (*Fig. 4*). From the 2000s to the 2010s, NDVI increased by 52.57% (*Table 1*). This may partly have been because China's national conservation policies have led to a substantial increase in forest area, enhancing their ability to capture more atmospheric C, directly promoting C sequestration capacity(Tang et al., 2018). The SOCD of an old forests ecosystem increased at an average rate of 0.61 kg C m^{-2} y^{-1} between 1979 and 2003 in southern China, indicating that old forests can remove C from the atmosphere(Zhou et al., 2006). A comprehensive global flux experiment also affirmed that old forests is an important C sink in terrestrial ecosystems, and has a rate of increase of 1.3 Pg C y^{-1}(Luyssaert et al., 2008). It is clear that surface soil C in the GKM region played a significant role as a C sink from 2000 to 2019, and that this may have partly been a result of the accumulation of natural C resulting from China's national conservation policies.

Another factor affecting the ability of forest to act as C sinks is the effect of climate change. The variations of temperature in growing season and inter annual in GKM have

http://www.aloki.hu ● ISSN 1589 1623 (Print) ● ISSN 1785 0037 (Online)
DOI: http://dx.doi.org/10.15666/aeer/2003_23032328

shown a significant increase trend from 2000 to 2019 ($P < 0.05$), whereas variations of precipitation decreased from 2000 to 2019 ($P > 0.05$, *Fig. 3*, *Fig. 4*). Climate warming has been accelerated as atmospheric CO_2 and soil nitrous oxide (N_2O) concentrations have risen, these changes may exacerbate global warming, which could enhance both vegetation growth and litter fall into soils, subsequently result in a soil C sink(Davidson and Janssens, 2006). Atmospheric CO_2 concentrations increased at a rate of 1.43 ppm y^{-1} in China (ppm = mg) from 1961 to 2005(Tian et al., 2011). Application of the process-based global vegetation model (DyN-LPJ) indicated that the decadal average N_2Oemissions in the 20thcentury ranged from 8.2 to 9.5 Tg N y^{-1}(Xu-Ri et al., 2012). GKM has been found to be very sensitive to climate change, as it has a short, warm summer and a long, cold winter that lasts for 9 months (Xu, 1998). Simultaneous heat and precipitation in summer are beneficial to vegetation growth under conditions of climate warming. The long cold season is beneficial to the input of external C which offsets the C lost by soil respiration, and thus the function of a C sink is established.

Uncertain analysis

The SOCD estimated based on NDVI (11.60 ±0.0001Kg C m^{-2}, 2000s; 14.17±0.0001 Kg C m^{-2}, 2010s) was higher than that based on field survey (9.15±0.36 Kg C m^{-2}(Xu et al., 2018a), 2000s; 10.64±0.83 Kg C m^{-2}, 2010s) in the two periods. It is generally believed that satellite-based estimation of SOCD can effectively reduce uncertainties caused by soil spatial heterogeneity. The difference of estimation in this paper may be due to the uneven spatial distribution of sampling points in the two periods. In 2010s, the sampling points were set according to the system sampling method through the geographical grid of 0.5°×0.5°, and the distribution was relatively uniform. However, due to the limitation of historical published data, the location distribution of sampling points in 2000s is not uniform. The regression relationship used to generate SOCD may cause potential uncertainty.

In order to overcome this difference, buffer analysis was carried out based on the sample location of 2000s to minimize the error caused by terrain inconsistency caused by different sampling locations. The ANOVA results showed that when r= 0.5°, 0.8° and 1°, the average SOCD of 2010s is significantly higher than 2000s ($P < 0.05$, *Table A4*). Therefore, we believe that the difference between the positions of different same points is within the allowable range of error, that is, the change of the two periods is due to the increase of forest vegetation area and the recovery of above-ground vegetation in the past 20 years. In addition, due to the widespread low temperature season and the distribution of large permafrost in GKM region, the soil properties are relatively stable (Baumann et al., 2009).

Impact factors of SOCD

Many field data were used to compare the effects of biotic and abiotic factors on SOCD spatial distribution in different forests types in GKM. Consistent with general theories and empirical experiments, RDA analysis showed that both biotic and abiotic factors affected the spatial pattern of SOCD in the surface soil of GKM (*Fig. 9*). Of these, climate (MAT, MAP), under vegetation diversity indices (Shannon-Wiener indices, Simpson indices) and site (Alt) had a significant influence ($P < 0.05$). The effects of biotic and abiotic factors on SOCD varied greatly in different types of forest. Multiple regression analysis clearly showed the influence of climate and the under vegetation diversity indices on SOCD spatial distribution in DNF and DBF, and climate (MAP, MGP) was higher

http://www.aloki.hu ● ISSN 1589 1623 (Print) ● ISSN 1785 0037 (Online)
DOI: http://dx.doi.org/10.15666/aeer/2003_23032328

than under vegetation diversity indices (*Fig. 10*). This is consistent with studies showing that the large scale spatial distribution pattern of SOCD is mainly regulated by climate (Post et al., 1982; Yang et al., 2007). However, the explanatory ability of temperature on SOCD was lower than that of precipitation in DNF and DBF (*Fig. 10*), and the dominant advantage of precipitation was more significant in DBF ($P < 0.05$). This is contrary to the traditional theory that the pattern of spatial distribution of forest SOCD is mainly controlled by C loss resulting from soil microbial heterorespiration under conditions of global warming(Valentini et al., 2000). Recent studies also show that the C density of *Piceaasperata* Mast. and *Abiesfabri* Mast. is mainly controlled by temperature on the Tibetan Plateau(Jia et al., 2021). In our results, high precipitation had a greater ability to explain SOCD (*Fig. 10*). MAP had a positive effect on SOCD, indicating that precipitation promotes the input of C into soil by vegetation and litter in DNF, thereby increasing SOCD. MAP had a negative effect on SOCD, and this may have been because soil rock fragment content is higher in DBF than in DNF; the SOC may have been washed away following high precipitation, leading to leaching in DBF(Lin et al., 2016).

Multiple regression analysis showed that the under vegetation diversity indices had a greater ability to explain the SOCD spatial pattern in DBF than in DNF ($P < 0.05$, *Fig. 10*). The consistently positive effects found in the current study were corroborated by our investigation, which showed that higher under vegetation diversity increases soil C inputs such as aboveground net primary productivity and belowground biomass(Liang et al., 2016; Liu et al., 2021), and promotes soil microbial community diversity and activity. The increased SOCD may originate from suppressed C loss from microbial decomposition (Rasse et al., 2005; Chen et al., 2018).

High soil pH had a negative effect on SOCD in all three forests types in GKM, and was significant in BNMF ($P < 0.05$, *Fig. 10*). The effect of high soil pH on SOCD may impact soil C input by regulating the diversity and productivity of aboveground vegetation (Chen et al., 2018). High soil acidity enhanced SOCD by limiting soil microbial vitality and expediting the movement of dissolved organic C eluviate into the deep layer (Funakawa et al., 2014). High levels of nitrogen deposition will also lead to soil acidification, but C retention caused by nitrogen deposition may be offset by the balance of greenhouse gases (CO_2 and N_2O etc.), resulting in a heating effect on the climate (Qu et al., 2020).

In contrast to the traditional view, we investigated the long term effects of climate factors on SOCD from 2000 to 2019 at the grid level, and found the influence of MAP was higher than MAT on SOCD (*Fig. 11*). A simulation study has shown that climate warming significantly enhanced ecosystem C sinks in spring during 1980 to 1989, but it was clear that this occurrence was reduced at the beginning of the 2000s (Piao et al., 2017). Giardina and Ryan (2000)showed that soil microbial activity did not change significantly under experimental conditions of temperature limitation, and decomposition did not change significantly when only temperature was increased. In this study, MAP was found to have a strong effect on SOCD in GKM forests (*Fig. 11*). Decomposition may be controlled by precipitation rather than by low temperatures, because of the long cold season, and by the large area of permafrost in the GKM(Baumann et al., 2009). GKM is located on the 400 mm precipitation line in China. The east side of the ridge is affected by the southeastern monsoon and experiences more than 400 mm precipitation annually. The west side of the ridge is affected by the Mongolia Siberia airflow, and so is drier and cooler than the east side(Xu, 1998). Soil moisture restricts microbial activities more than soil temperature in an arid soil environment, thus controlling soil C dynamics (Lin et al.,

http://www.aloki.hu ● ISSN 1589 1623 (Print) ● ISSN 1785 0037 (Online)
DOI: http://dx.doi.org/10.15666/aeer/2003_23032328

2016; Přívětivý and Šamonil, 2021). Therefore, using MAP as a key factor in the development of large scale models will be of significance in assessing C dynamics in GKM in the future.

Conclusions

The SOCD estimated based on NDVI (11.60 ±0.0001Kg C m^{-2}, 2000s; 14.17±0.00001 Kg C m^{-2}, 2010s) was significantly higher than that based on field survey (9.15 ± 0.36 Kg C m^{-2}(Xu et al., 2018a), 2000s; 10.64±0.83 Kg C m^{-2}, 2010s), illustrating a rate of increase of 0.15 ±0.05 kg C m^{-2} y^{-1} from 2000 to 2019. These data provided a benchmark for exploration of the dynamic effects of climate warming on the soil C of a boreal forest ecosystem in the northeastern cold temperate zone. The SOCD exhibited a strong correlation with under vegetation diversity in terms of spatial distribution, and this indicated that conservation of biodiversity promotes regional forest C sequestration. This study validated the plant diversity-soil C storage hypothesis on a broad spatial scale. Our results also demonstrated the critical role of MAP in shaping SOCD dynamics across the GKM from 2000 to 2019, suggesting that the linkage between soil C uptake and temperature is unstable in northern ecosystems. Data on SOCD were limited, however, and it was unclear whether the significant inter-annual correlation between SOCD and precipitation reflected inter-decadal changes, and whether long term changes have taken place in the ecological response to climate warming in boreal forest ecosystems. Further research is needed into longer term observations, using more focused analysis of soil C dynamics, to simulate C-climate feedback in regions of major soil organic C storage.

Acknowledgements. We would like to thank the members of the field investigators, and Drs. Bing Wang, Zhunxia Zhang, Fangjian Yang and Chao Zhang for their assistance in the soil sample collection and laboratory. This research was funded by Inner Mongolia Autonomous Region Science and Technology Plan Project: Research and Demonstration on Key Technologies of Ecological Restoration of Betula platyphylla Secondary Forest in Greater Khingan Mountains, grant number 2020GG0067, and the Inner Mongolia Autonomous Region Graduate Education Innovation Program (Graduate Research Innovation Funding Project, 2020): Dynamics of Soil Carbon Density and its Influencing Factors in the Greater Khingan Mountains of Northeast China, grant number BZ2020049.

Conflicts of Interests. The authors have no conflicts of interests to disclose.

REFERENCES

[1] Baumann, F., He, J.S., Schmidt, K., Kühn, P., Scholten, T. (2009): Pedogenesis, permafrost, and soil moisture as controlling factors for soil nitrogen and carbon contents across the Tibetan Plateau. – Global Change Biology 15 (12): 3001-3017. https://doi.org/10.1111/j.1365-2486.2009.01953.x.

[2] Bonan, G. B. (2008): Forests and climate change: forcings, feedbacks, and the climate benefits of forests. – Science 320: 1444-1449. https://doi.org/10.1126/science.1155121.

[3] Bossio, D.A., Cook-Patton, S.C., Ellis, P.W. (2020): The role of soil carbon in natural climate solutions. – Nat Sustain3: 391-398. https://doi.org/10.1038/s41893-020-0491-z.

[4] Bray, R. H., Kurtz, L. T. (1945): Determination of total, organic, and available forms of phosphorus in soils. – Soil Science59(1): 39-46.https://doi.org/10.1097/00010 694-194501000-00006.

[5] Bull, G.Q., Nilsson, S. (2004): An Assessment of China's Forest Resources. – International Forestry Review 6(3): 210-220. https://doi.org/10.1505/ifor.6.3.210.59979.

http://www.aloki.hu ● ISSN 1589 1623 (Print) ● ISSN 1785 0037 (Online)
DOI: http://dx.doi.org/10.15666/aeer/2003_23032328

[6] Chen, T., Zang, J. (1999): A comparation of fifteen species diversity indices. – HeNan Science 17: 56-57.
[7] Chen, L., Liang, J., Qin, S., Liu, L., Fang, K., Xu, Y., Ding, J., Li, F., Luo, Y., Yang, Y. (2016): Determinants of carbon release from the active layer and permafrost deposits on the Tibetan Plateau. – Nature Communications 7: 1-12. https://doi.org/10.1038/ncomms13046.
[8] Chen, S., Wang, W., Xu, W., Wang, Y., Wan, H., Chen, D., Tang, Z., Tang, X., Zhou, G., Xie, Z., Zhou, D., Shangguan, Z., Huang, J., He, J.S., Wang, Y., Sheng, J., Tang, L., Li, X., Dong, M., Wu, Y., Wang, Q., Wang, Z., Wu, J., Chapin III, F.S., Bai, Y. (2018): Plant diversity enhances productivity and soilcarbon storage. – PNAS 115(16): 4027-4032. https://doi.org/10.1073/pnas.1700298114.
[9] Chinese Academy of Sciences. (2001): Vegetation Atlas of China. – SciencePress, Beijing.
[10] Crowther, T.W., van den Hoogen, J., Wan, J., Mayes, M.A., Keiser, A.D., Mo, L., Averill, C., Maynard, D.S. (2019): The global soil community and its influence on biogeochemistry. – Science 365(6455). https://doi.org/10.1126/science.aav0550.
[11] Davidson, E.A., Janssens, I.A. (2006): Temperature sensitivity of soil carbon decomposition and feedbacks to climate change. – Nature 440(7081): 165-173. https://doi.org/10.1038/nature04514.
[12] DFPRC (2014): Statistics of China's Forest Resources (2009-13). – Department of Forestry of PR China, Beijing, China 25-31. https://doi.org/10.1016/S0378-1127(02)00299-2.
[13] Ding, J.Z., Li, F., Yang, G.B., Chen, L.Y., Zhang, B.B., Liu, L., Fang, K., Qin, S.Q., Chen, Y.L., Peng, Y.F., Ji, C.J., He, H.L., Smith, P., Yang, Y.H. (2016): The permafrost carbon inventory on the Tibetan Plateau: a new evaluation using deep sediment cores. – Global Change Biology 22(8): 2688-2701. https://doi.org/10.1111/gcb.13257.
[14] Fang, J., Guo, Z., Piao, S., Chen, A. (2007): Terrestrial vegetation carbon sinks in China, 1981–2000. – Science in China Series D: Earth Sciences 50(9): 1341-1350. https://doi.org/10.1007/s11430-007-0049-1.
[15] Fang, J., Shen, Z., Tang, Z., Wang, X., Wang, Z., Feng, J., Liu, Y., Qiao, X., Wu, X., Zheng, C. (2012): Forest community survey and the structural characteristics of forests in China. – Ecography 35(12): 1059-1071. 1059-1071. https://doi.org/10.2307/23409648.
[16] Fang, Y., Michalak, A.M., Schwalm, C.R., Huntzinger, D.N., Berry, J.A., Ciais, P., Piao, S., Poulter, B., Fisher, J.B., Cook, R.B., Hayes, D., Huang, M., Ito, A., Jain, A., Lei, H., Lu, C., Mao, J., Parazoo, N.C., Peng, S., Ricciuto, D.M., Shi, X., Tao, B., Tian, H., Wang, W., Wei, Y., Yang, J. (2017): Global land carbon sink response to temperature and precipitation varies with ENSO phase. – Environmental Research Letters 12(6): 064007. https://doi.org/10.1088/1748-9326/aa6e8e.
[17] Fu, Y., He, H.S., Zhao, J., Larsen, D.R., Zhang, H., Sunde, M.G., Duan, S. (2018): Climate and Spring Phenology Effects on Autumn Phenology in the Greater Khingan Mountains, Northeastern China. – Remote Sensing of Environment 10(3): 449. https://doi.org/10.3390/rs10030449.
[18] Funakawa, S., Fujii, K., Kadono, A., Watanabe, T., Kosaki, T. (2014): Could Soil Acidity Enhance Sequestration of Organic Carbon in Soils? – In: Hartemink, A., McSweeney, K. (eds.) Soil Carbon - Progress in Soil Science. Springer, Cham. https://doi.org/10.1007/978-3-319-04084-4_22.
[19] Giardina, C., Ryan, M. (2000): Evidence that decomposition rates of organic carbon in mineral soil do not vary with temperature. – Nature 404: 858-861.https://doi.org/10.1038/35009076.
[20] Gocic, M., Trajkovic, S. (2013): Analysis of changes in meteorological variables using Mann-Kendall and Sen's slope estimator statistical tests in Serbia. – Global and planetary change 100:172-182. https://doi.org/10.1016/j.gloplacha.2012.10.014.
[21] Guo, Z., Hu, H., Li, P., Li, N., Fang, J. (2013): Spatio-temporal changes in biomass carbon sinks in China's forests from 1977 to 2008. – Sci China Life Sci 56(7): 661-671. https://doi.org/10.1007/s11427-013-4492-2.

http://www.aloki.hu ● ISSN 1589 1623 (Print) ● ISSN 1785 0037 (Online)
DOI: http://dx.doi.org/10.15666/aeer/2003_23032328

[22] He, J.S. (2012): Carbon cycling of Chinese forests: from carbon storage, dynamics to models. – Science China Life Sciences 55: 188-190. https://doi.org/10.1007/s11427-012-4285-z.
[23] Holben, B.N. (1986): Characteristics ofmaximum-value composite images from temporal AVHRR data. – InternationalJournal of Remote Sensing 7(11): 1417-1434. https://doi.org/10.1080/01431168608948945.
[24] Hopkins, F.M., Torn, M.S., Trumbore, S.E. (2012): Warming accelerates decomposition of decades-old carbon in forest soils. – Proceedingsof the National Academy of Sciences of the United States of America 109(26): 1753-1761. https://doi.org/10.1073/pnas.1120603109.
[25] Hou, X. (2019): 1:1 million vegetation map of China. – National Tibetan Plateau Data Center. http://data.tpdc.ac.cn.
[26] Jia, L., Wang, G., Lou, J. (2021): Carbon storage of the forest and its spatial pattern in Tibet, China. – Journal of Mountain Science 18(7): 1748-1761. https://doi.org/10.1007/s11629-020-6520-6.
[27] Jiang, H., Apps, M., Peng, C., Zhang, Y., Liu, J. (2002): Modelling the influence of harvesting on Chinese boreal forest carbon dynamics. – For Ecol Manage 169: 65-82. https://doi.org/10.1016/S0378-1127(02)00299-2.
[28] Liang, J., Crowther, T.W., Picard, N., Wiser, S., Zhou, M. (2016): Positive biodiversity-productivity relationship predominant in global forests. – Science 354(6309): 196-200. https://doi.org/10.1126/science.aaf8957.
[29] Lin, L., Zhu, B., Chen, C., Zhang, Z., Wang, Q.-B., He, J.-S. (2016): Precipitation overrides warming in mediating soil nitrogen pools in an alpine grassland ecosystem on the Tibetan Plateau. – Scientific Report 6: 1-9. https://doi.org/10.1038/srep31438.
[30] Liu, Z. (2017): Variation characteristics and trend of precipitation over the Shangsha river basin. – Anhui Agricultural Science Bulletin.
[31] Liu, Y., Yue, C., Wei, X., Blanco, J.A., Trancoso, R. (2020): Tree profile equations are significantly improved when adding tree age and stocking degree: an example for Larixgmelinii in the Greater Khingan Mountains of Inner Mongolia, northeast China. – European Journal of Forest Research 139(3): 443-458. https://doi.org/10.1007/s10342-020-01261-z.
[32] Liu, Y., Shangguan, Z., Deng, L. (2021): Vegetation Type and Soil Moisture Drive Variations in Leaf Litter Decomposition Following Secondary Forest Succession. – Forests 12(9): 1195. https://doi.org/10.3390/f12091195.
[33] Luyssaert, S., Schulze, E., Börner, A. (2008): Old-growth forests as global carbon sinks. – Nature 455: 213-215. https://doi.org/10.1038/nature07276.
[34] Mao, D., He, X., Wang, Z., Tian, Y., Xiang, H., Yu, H., Man, W., Jia, M., Ren, C., Zheng, H. (2019): Diverse policies leading to contrasting impacts on land cover and ecosystem services in Northeast China. – Journal of Cleaner Production 240: 1-11. https://doi.org/10.1016/j.jclepro.2019.117961.
[35] Meng, X., Liu, Q., Tao, L., Deng, L., Li, W., Wen, Z. (2014): Carbon storage of young and middle age forest in south and north Daxing'anling mountains. – Journal of Central South University of Forestry & Technology 34(6): 37-43. https://doi.org/1673-923X(2014)06-0037-07.
[36] Ministry of ecology and environment of the people' s Republic of China. (2021): Technical specification for investigation and assessment of national ecological status - Field observation of forest ecosystem.
[37] Pan, Y., Birdsey, R.A., Fang, J., Houghton, R. (2011): A Large and Persistent Carbon Sink in the World's Forests. – Science 333(6045): 988-993. https://doi.org/10.1111/j.1469-8137.2011.03645.x.
[38] Piao, S., Fang, J., Zhou, L., Ciais, P., Zhu, B. (2006): Variations in satellite-derived phenology in China's temperate vegetation. – GlobalChange Biology 12: 672-685. https://doi.org/10.1111/j.1365-2486.2006.01123.x.

http://www.aloki.hu ● ISSN 1589 1623 (Print) ● ISSN 1785 0037 (Online)
DOI: http://dx.doi.org/10.15666/aeer/2003_23032328

[39] Piao, S., Liu, Z., Wang, T., Peng, S., Ciais, P., Huang, M., Ahlstrom, A., Burkhart, J.F., Chevallier, F., Janssens, I.A., Jeong, S.-J., Lin, X., Mao, J., Miller, J., Mohammat, A., Myneni, R.B., Peñuelas, J., Shi, X., Stohl, A., Yao, Y., Zhu, Z., Tans, P.P. (2017): Weakening temperature control on the interannual variations of spring carbon uptake across northern lands. – Nature Climate Change 7(5): 359-363. https://doi.org/10.1038/nclimate3277.

[40] Post, W.M., Emanuel, W.R., Zinket, P.J., Stangenberger, A.G. (1982): Soil carbon pools and world life zones. – Nature 298: 156-159. https://doi.org/10.1038/298156a0.

[41] Přívětivý, T., Šamonil, P. (2021): Variation in Downed Deadwood Density, Biomass, and Moisture during Decomposition in a Natural Temperate Forest. – Forests 12(10): 1352. https://doi.org/10.3390/f12101352.

[42] Qu, S., Xu-Ri, Yu, J., Li, F., Wei, D., Borjigidai, A. (2020): Nitrogen deposition accelerates greenhouse gas emissions at an alpine steppe site on the Tibetan Plateau. – Science of the Total Environment 765(1): 144277. https://doi.org/10.1016/j.scitotenv.2020.144277.

[43] Rasse, D.P., Rumpel, C., Dignac, M.-F. (2005): Is soil carbon mostly root carbon? Mechanisms for a specific stabilisation. – Plant and Soil 269: 341-356. https://doi.org/10.1007/s11104-004-0907-y.

[44] Schimel, D. S., Braswell, B.H., Holland, E.A., McKeown, R., Ojima, D.S., Painter, T., Parton, W.J., Townsend, A.R. (1994): Climatic, edaphic, and biotic controls over storage and turnover of carbon in soils. – Global Biogeochemical Cycles 8: 279-293. https://doi.org/10.1029/94GB00993.

[45] Schmidt, C. O., Ittermann, T., Schulz, A., Grabe, H. J., Baumeister, S. E. (2013): Linear, nonlinear or categorical: how to treat complex associations in regression analyses? polynomial transformations and fractional polynomials. – International Journal of Public Health58(1): 157-160. https://10.1007/s00038-012-0363-z.

[46] Seenu, P. Z., Jayakumar, K. V. (2021): Comparative study of innovative trend analysis technique with Mann-Kendall tests for extreme rainfall. – Arabian Journal of Geosciences 14(7): 536. https://doi.org/10.1007/s12517-021-06906-w.

[47] Shen, M.G., Piao, S.L., Jeong, S.J., Zhou, L.M., Zeng, Z.Z., Ciais, P., Chen, D.L., Huang, M.T., Jin, C.S., Li, L.Z., Li, Y., Myneni, R.B., Yang, K., Zhang, G.X., Zhang, Y.J., Yao, T.D. (2015): Evaporative cooling over the Tibetan Plateau induced by vegetation growth. – Proceedings of the NationalAcademy of Sciences of the United States of America 112: 9299-9304. https://doi.org/10.1073/pnas.1504418112.

[48] Tang, X., Zhao, X., Bai, Y., Tang, Z., Wang, W., Zhao, Y., Wan, H., Xie, Z., Shi, X., Wu, B., Wang, G., Yan, J., Ma, K., Du, S., Li, S., Han, S., Ma, Y., Hu, H., He, N., Yang, Y., Han, W., He, H., Yu, G., Fang, J., Zhou, G. (2018): Carbon pools in China's terrestrial ecosystems: New estimates based on an intensive field survey. – PNAS 115(16): 4021-4026. https://doi.org/10.1073/pnas.1700291115.

[49] Tharammal, T., Bala, G., Devaraju, N., Nemani, R. (2019): A review of the major drivers of the terrestrial carbon uptake: model-based assessments, consensus, and uncertainties. – Environmental Research Letters 14(9): 093005. https://doi.org/10.1088/1748-9326/ab3012.

[50] Tian, H., Melillo, J., Lu, C., Kicklighter, D., Liu, M., Ren, W., Xu, X., Chen, G., Zhang, C., Pan, S., Liu, J., Running, S. (2011): China's terrestrial carbon balance: Contributions from multiple global change factors. – Global Biogeochemical Cycles 25(1): 1-16. https://doi.org/10.1029/2010GB003838.

[51] Tucker, C.J., Pinzon, J.E., Brown, M. E. (2004): Global Inventory Modeling and Mapping Studies. – Global Land Cover Facility, University of Maryland.

[52] Tucker, C.J., Pinzon, J.E., Brown, M. E., Slayback, D., Pak, E. W., Mahoney, R., Vermote, E., El Saleous, N. (2005): An Extended AVHRR 8-km NDVI Data Set Compatible with MODIS and SPOT Vegetation NDVI Data. – International Journal of Remote Sensing 26: 4485-4498.

http://www.aloki.hu ● ISSN 1589 1623 (Print) ● ISSN 1785 0037 (Online)
DOI: http://dx.doi.org/10.15666/aeer/2003_23032328

[53] Valentini, R., Matteucci, G., Dolman, A.J., Schulze, E.-D., Rebmann, C., Moors, E.J. (2000): Respiration as themain determinant of carbonbalance in European forests. – Nature 404: 861-865. https://doi.org/10.1038/35009084.
[54] Wu, H. (2015): Comparative study of species diversity indices of different type communities. – Journal of Central South University of Forestry & Technology 35(5): 84-89.
[55] Xu, H. (1998): Forests in Greater Khingan Mountains, China. – Science PressBeijing, China, pp. 3-6.
[56] Xu, L., He, N., Yu, G. (2018a): 2010s China Land Ecosystem Carbon Density Dataset. – Science Data Bank 4(1). https://doi.org/10.11922/csdata.2018.0026.zh; Data DOI: https://doi.org/10.11922/sciencedb.603.
[57] Xu, L., Yu, G., He, N., Wang, Q., Gao, Y., Wen, D., Li, S., Niu, S., Ge, J. (2018b): Carbon storage in China's terrestrial ecosystems: A synthesis. – Scientific Reports 8(2806): 1-13. https://doi.org/10.1038/s41598-018-20764-9.
[58] Xu-Ri, Prentice, I.C., Spahni, R., Niu, H.S. (2012); Modelling terrestrial nitrous oxide emissions and implications for climate feedback. – New Phytologist 196(2): 472-488. https://doi.org/10.1111/j.1469-8137.2012.04269.x.
[59] Yang, Y., Mohammat, A., Feng, J., Zhou, R., Fang, J. (2007): Storage, patterns and environmental controls of soil organic carbon in China. – Biogeochemistry 84: 131-141. https://doi.org/10.1007/s10533-007-9109-z.
[60] Yang, Y., Fang, J., Tang, Y., Ji, C., Zheng, C., He, J., Zhu, B. (2008): Storage, patterns and controls of soil organic carbon in the Tibetan grasslands. – GlobalChange Biology 14(7): 1592-1599. https://doi.org/10.1111/j.1365-2486.2008.01591.x.
[61] Yang, Y., Fang, J., Smith, P., Tang, Y., Chen, A., Ji, C., Hu, H., Rao, S., Tan, K., He, J.-S. (2009): Changes in topsoil carbon stock in the Tibetan grasslands between the 1980s and 2004. – Global Change Biology 15(11): 2723-2729. https://doi.org/10.1111/j.1365-2486.2009.01924.x.
[62] Yang, Y.H., Luo, Y.Q., Finzi, A.C. (2011): Carbon and nitrogen dynamics during forest stand development: a global synthesis. – New Phytologist 190(4): 977-989. https://doi.org/10.1111/j.1469-8137.2011.03645.x.
[63] Yang, Y., Wang, G., Shen, H., Yang, Y., Cui, H., Liu, Q. (2014a): Dynamics of carbon and nitrogen accumulation and C:N stoichiometry in a deciduous broadleaf forest of deglaciated terrain in the eastern Tibetan Plateau. – Forest Ecologyand Management 312: 10-18. https://doi.org/10.1016/j.foreco.2013.10.028.
[64] Yang, Y.H., Li, P., Ding, J.Z., Zhao, X., Ma, W.H., Ji, C.J., Fang, J.Y. (2014b): Increased topsoil carbon stock across China's forests. – Global Change Biology 20(8): 2687-2696. https://doi.org/10.1111/gcb.12536.
[65] Yang, Z., Chen, S., Liu, X., Xiong, D., Xu, C., Arthur, M.A., McCulley, R.L., Shi, S., Yang, Y. (2019): Loss of soil organic carbon following natural forest conversion to Chinese fir plantation. – Forest Ecology and Management 449: 117476. https://doi.org/10.1016/j.foreco.2019.117476.
[66] Zhang, T., Zhang, Q., Wang, Q. (2014): Model detection for functional polynomial regression. – Computational Statistics & Data Analysis70: 183-197. https://doi.org/10.1016/j.csda.2013.09.007.
[67] Zhang, C., Lu, D., Chen, X., Zhang, Y., Maisupova, B., Tao, Y. (2016): The spatiotemporal patterns of vegetation coverage and biomass of the temperate deserts in Central Asia and their relationships with climate controls. – Remote Sensing of Environment 175: 271-281. https://doi.org/10.1016/j.rse.2016.01.002.
[68] Zhang, Y., Yao, Y., Wang, X., Liu, Y., Piao, S. (2017): Mapping spatial distribution of forest age in China. – Earth and Space Science4(3): 108-116. https://doi.org/10.1002/2016EA000177.

http://www.aloki.hu ● ISSN 1589 1623 (Print) ● ISSN 1785 0037 (Online)
DOI: http://dx.doi.org/10.15666/aeer/2003_23032328

[69] Zhao, W., Li, F., Zhuang, C., Wang, S. (2014): Spatial Distribution of Carbon Density for Larch Forest in Daxing'an Mountain. – Journal of Northeast Forestry University 42(6): 1-5. https://doi.org/10.13759/j.cnki.dlxb.20140523.027.
[70] Zhou, G., Liu, S., Li, Z. (2006): Old-growth forests can accumulate carbon in soils. – Science 314: 1417. https://doi.org/10.1126/science.1130168.
[71] Zhu, K. (1996): China soil species description. – National Soil Survey Office, China Agriculture Press, Beijing, China. ISBN: 9787109040014. (in Chinese).
[72] Zhu, J., Wang, C., Zhou, Z., Zhou, G., Hu, X., Jiang, L., Li, Y., Liu, G., Ji, C., Zhao, S., Li, P., Zhu, J., Tang, Z., Zheng, C., Birdsey, R.A., Pan, Y., Fang, J. (2020): Increasing soil carbon stocks in eight permanent forest plots in China. – Biogeosciences 17(3): 715-726. https://doi.org/10.5194/bg-17-715-2020.

http://www.aloki.hu ● ISSN 1589 1623 (Print) ● ISSN 1785 0037 (Online)
DOI: http://dx.doi.org/10.15666/aeer/2003_23032328

APPENDIX

Table A1. *Information of the sampling points*

Sample sites	Longitude (°E)	Latitude (°N)	Altitude (m)	Slope (°)	aspect
1	123.5555	53.3491	384.5	11	NE
2	125.2366	53.0775	241.9	4	S
3	125.6913	52.9904	233.4	2	NE
4	125.0161	52.5054	368.3	7	NS
5	125.8554	52.4578	370.6	2	NS
6	126.2322	52.1672	365.9	2	N
7	120.0591	52.7695	451.3	14	N
8	120.8355	52.5942	464.7	24	SE
9	123.2463	52.2147	637.9	3	SW
10	125.7564	51.9425	359.8	3	NE
11	122.2076	51.7776	838.3	11	SW
12	123.8825	51.6108	721.0	3	NW
13	124.6865	51.5411	560.5	3	NE
14	121.5112	50.9352	589.7	10	SW
15	121.2882	51.3818	1009.8	12	E
16	123.9258	51.0470	563.8	3	NW
17	124.4692	50.9044	548.7	2	NW
18	125.3149	50.8160	435.8	5	NW
19	119.8033	50.6746	635.8	15	NW
20	121.1850	50.8286	791.8	18	S
21	122.7866	50.6547	606.4	2	NS
22	123.5743	50.5033	453.1	3	NE
23	124.3528	50.4060	437.1	20	NS
24	122.0220	47.6090	467.9	22	E
25	120.2438	50.3773	707.2	10	N
26	120.8675	50.3724	660.7	6	SW
27	121.8085	50.1454	908.7	20	SE
28	122.5167	50.1199	572.6	1	S
29	123.3901	50.0371	439.7	15	S
30	124.2128	49.9079	334.6	6	NE
31	121.3788	47.5316	610.8	18	NE
32	120.6427	47.5263	1087.7	12	NE
33	119.9947	47.3310	945.8	26	N
34	120.7520	49.9117	839.1	8	N
35	121.6310	49.6524	758.6	13	S
36	122.4485	49.5209	590.8	2	SE
37	124.0619	49.3260	392.1	5	NW
38	121.2396	47.9531	755.6	11	N
39	120.5106	48.0737	919.3	6	NE
40	119.9517	48.2030	822.7	9	NW
41	120.7081	49.1771	764.0	25	NE

http://www.aloki.hu ● ISSN 1589 1623 (Print) ● ISSN 1785 0037 (Online)
DOI: http://dx.doi.org/10.15666/aeer/2003_23032328

Sample sites	Longitude (°E)	Latitude (°N)	Altitude (m)	Slope (°)	aspect
42	121.3836	49.0670	773.4	26	N
43	122.2989	48.9663	261.2	9	N
44	123.3565	49.0451	372.5	3	SE
45	123.8718	48.7824	291.2	8	S
46	121.3363	48.5146	997.0	10	W
47	122.0335	47.8940	533.0	6	NE
48	121.5556	51.1339	850.2	12	S
49	122.4342	50.9908	741.5	22	S
50	122.4336	50.9903	498.5	8	S
51	122.4331	50.9903	855.5	23	E
52	122.0917	50.9439	436.3	3	NE
53	122.0936	50.9419	972.8	4	NE
54	122.0903	50.9461	855.5	23	E
55	122.0875	50.9511	502.0	7	SE
56	122.3608	50.9931	403.8	15	NW
57	121.5053	50.9397	822.5	9	SE
58	121.5056	50.9233	829.4	6	S
59	121.4922	50.9397	483.2	6	NW
60	121.5214	50.8976	742.2	11	SE
61	121.5207	50.9118	571.5	6	SW
62	121.5224	50.9135	590.4	23	SE
63	122.2867	52.2862	907.0	5	SE
64	122.2881	52.2754	819.7	7	S
65	122.2865	52.2868	898.0	8	NE
66	121.9091	51.8886	676.0	7	S
67	121.9034	51.8751	797.8	10	S
68	121.9042	51.8765	843.5	12	S

Table A2. *Changes in soil organic carbon density (SOCD, kg C m^{-2}) and soil carbon storage (SCS,Tg C) at 0-20 cm depth (at a 95% confidence interval) from the 2000s to the 2010s across the Greater Khingan Mountains*

	Area (10^4 m^2)	**Mean SOCD/SE (Kg C m^{-2})**		**Change in SOCD /SE**		**Change in SCS**
		2000s	2010s	(g C m^{-2} yr^{-1})	% yr^{-1}	(Tg C yr^{-1})
ALL-GKM	31.79	9.15/0.36	10.64/0.83	0.15/0.05*	0.16	0.48
DBF	11.78	10.59/0.74	13.95/1.35	0.34/0.12*	0.32	0.40
BNMF	1.55	8.38/0.53	10.94/2.05	0.26/0.15	0.31	0.04
DNF	18.46	8.63/0.56	8.89/1.10	0.03/0.009	0.03	0.06

ALL-GKM, all of the Greater Khingan Mountains; DBF, deciduous broadleaved forests; BNMF, broadleaf and needleleaf mixed forests; DNF, deciduous needleleaf forests. "*" represent the statistical test is significant ($P < 0.05$)

http://www.aloki.hu ● ISSN 1589 1623 (Print) ● ISSN 1785 0037 (Online)
DOI: http://dx.doi.org/10.15666/aeer/2003_23032328

Table A3. *multiple linear regression between soil organic carbon density and MAP and MAT in two periods, based on normalized difference vegetation index estimation.(MAP, mean annual precipitation (mm); MAT, mean annual temperature (°C))*

	Intercept/SE	Estimate/SE		n
		MAP	MAT	
2000s	1.20E-15/0.08	0.29/0.01**	-0.24/0.01**	129
2010s	-3.23E-16/0.07	0.56/0.08***	-0.001/0.08	129

***, P < 0.001; **, 0.001< P <0.01, at a 95% confidence interval

Table A4. *Changes in soil organic carbon density (SOCD, kg C m^{-2}) based on normalized difference vegetation index (NDVI) estimation at 0-20 cm depth from the 2000s to the 2010s across the Greater Khingan Mountains*

SOCD	Min	Max	Mean/SE
2000s	2.46	17.18	11.60/0.0001
2010s	2.78	21.33	14.17/0.0001

Table A5. *Results of variance analysis of SOCD in different buffers*

Buffers	Period	SOCD (Kg C m^{-2})						ANOVA	
		N	Mean/SE	Conf. int		Min	Max	F	P
	2000s	107	9.10/0.49	8.14	10.07	0.77	39.09		
R1=0.5°	2010s	20	11.26/1.63	7.83	14.69	2.46	24.30	2.640	0.026*
R2=0.8°	2010s	39	11.39/1.07	9.25	13.56	2.34	28.22	4.906	0.018*
R3=1°	2010s	49	11.67/0.99	9.66	13.71	2.34	28.22	6.694	0.011*

Conf. int: at a 95% confidence interval; *: P<0.05

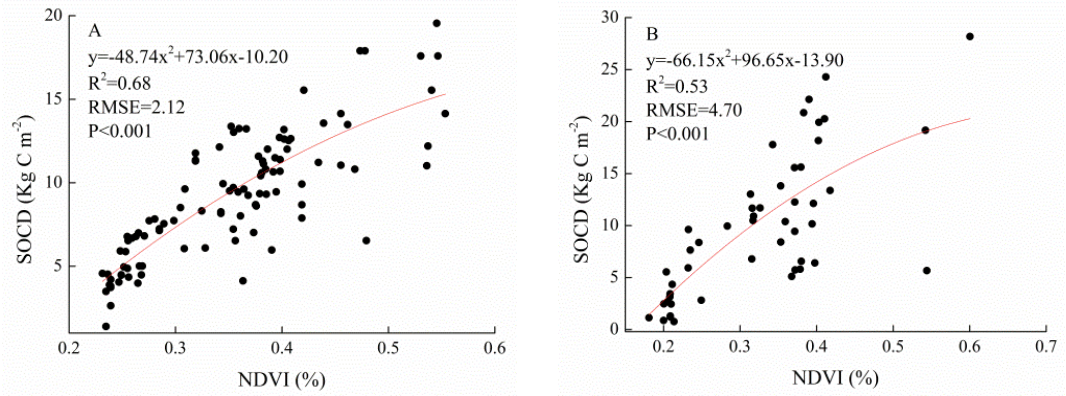

Figure A1.*Correlation between normalized difference vegetation index(NDVI) and soil organic carbon density (SOCD,kg C m^{-2}) in theGreaterKhinganMountainsforthe period of 2000s (A) and 2010s (B), derived from polynomial regression*

http://www.aloki.hu ● ISSN 1589 1623 (Print) ● ISSN 1785 0037 (Online)
DOI: http://dx.doi.org/10.15666/aeer/2003_23032328

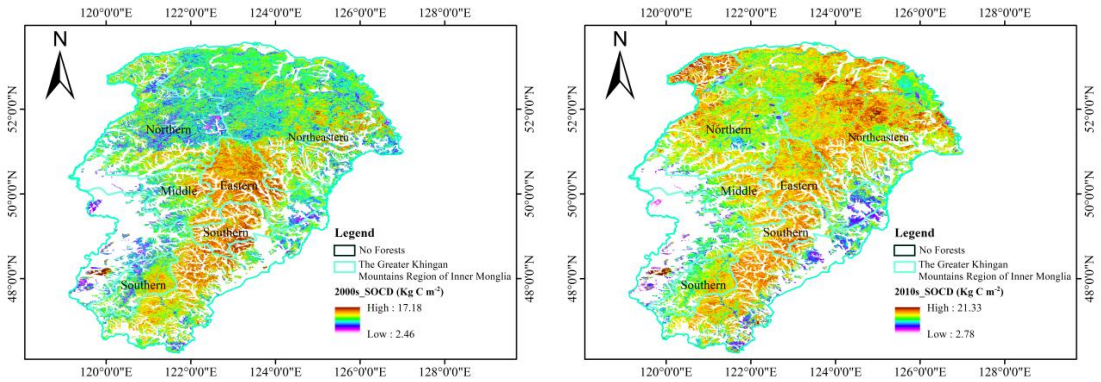

Figure A2. *Spatial distribution of soil organic carbon density (SOCD, kg C m^{-2}) based on normalized difference vegetation index (NDVI) estimation at 0-20 cm depth from the 2000s to the 2010s across the Greater Khingan Mountains*

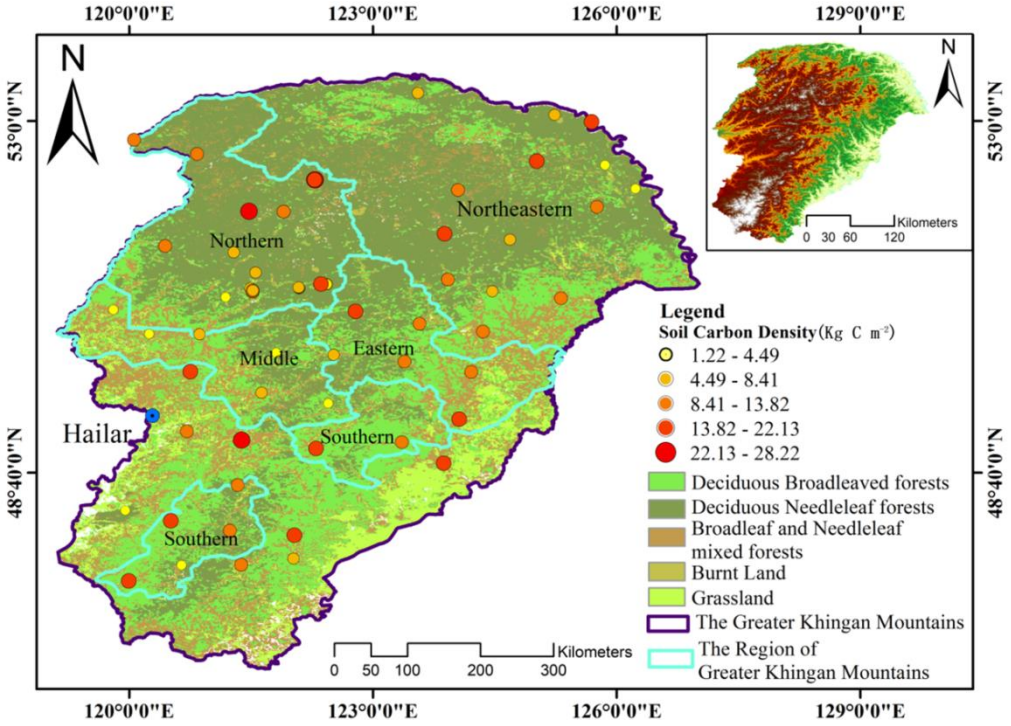

Figure A3. *Spatial distribution of soil organic carbon density (kg C m^{-2}) in the Greater Khingan Mountains*

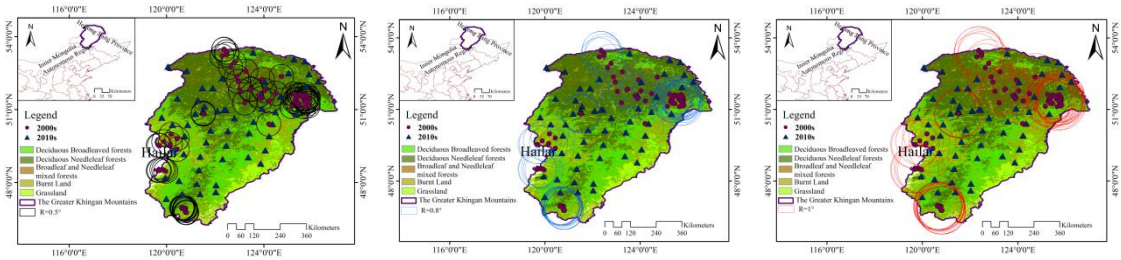

Figure A4. *Buffer overlap diagram of 2010S sample point and 2000s sample point (r = 0.5°, r = 0.8°, r = 1°)*

http://www.aloki.hu ● ISSN 1589 1623 (Print) ● ISSN 1785 0037 (Online)
DOI: http://dx.doi.org/10.15666/aeer/2003_23032328